

# Cu isotopes in groundwater for hydrogeochemical mineral exploration: A case study using the world-class Mount Isa Cu–Pb–Zn deposit (Australia)

B. Mahan<sup>a,b,\*</sup>, R. Mathur<sup>c</sup>, I. Sanislav<sup>b</sup>, P. Rea<sup>d</sup>, P. Dirks<sup>b</sup>

<sup>a</sup> IsoTropics Geochemistry Lab, Earth and Environmental Science, James Cook University, Townsville, QLD, Australia

<sup>b</sup> Economic Geology Research Centre (EGRU), Earth and Environmental Science, James Cook University, Townsville, QLD, Australia

<sup>c</sup> Geology Department, Juniata College, Huntingdon, PA, USA

<sup>d</sup> Mount Isa Mines (MIM) / Glencore, Australia

## ARTICLE INFO

### Keywords:

Hydrogeochemistry  
Stable metal isotope geochemistry  
Mineral exploration  
Groundwater  
Critical metals  
Copper

## ABSTRACT

Copper is the crux resource in the transition to renewable energy sources, with green technologies such as solar panels, wind turbines and batteries all relying on this critical metal for their componentry, and more importantly for connection to electrical grids. While demand intensifies, copper discovery rates continue to fall due to increased scarcity of deposits that are outcropping and/or detectable by conventional means. This has engendered novel methods of detecting Cu-bearing ore under cover, such as hydrogeochemical analyses to trace ore mineral interaction with natural waters. This notably includes the development of Cu isotope systematics in natural waters, wherein proximal to Cu-bearing ore bodies enrichment of water in the heavier Cu isotope occurs (e.g. from oxidative weathering), thus providing a fingerprint of water interaction with Cu-bearing sulfides. Here, Cu isotope compositions for eighteen groundwater samples overlying and distal to the world-class, sediment-hosted stratiform Mount Isa Cu–Zn–Pb deposit were analyzed to assess the utility of groundwater Cu isotope compositions as an exploration tool for Cu-bearing ore under cover. A further 12 chalcopyrite Cu isotope compositions were determined from two drill cores directly overlying the main Cu-bearing ore body, to establish a baseline Cu isotope composition for the Mt Isa deposit. Cu isotope data were synthesized together with field water parameters and placed within a geological context to construct a framework for interpretation. When accounting for industrially impacted sites and underlying geology, results show a clear trend towards heavy Cu isotope enrichment in groundwater proximal to known mineralization, with enrichments of ~1 per mil (‰) or more relative to distal groundwater and primary deposit chalcopyrite. These results corroborate and expand upon similar work from surface and groundwater samples around porphyry, exotic and IOCG Cu-bearing deposits. Moreover, these results strongly indicate that groundwater Cu isotope systematics for exploration under cover has great potential as a vectoring tool, illustrating that thus far the technique is applicable across deposit types.

## 1. Introduction

Copper is one of the most ubiquitous and widely used metals in modern civilization and is a key resource in the economic sector (e.g. for grid infrastructure, plumbing, transportation and electronics). Notably, Cu is in many ways *the* crux metal in the transition to more sustainable societies, as it is pivotal in the further development and implementation of “green energy solutions” (Elshkaki et al., 2016; WorldBank, 2021). Due to its inherent necessity for modern and future societies—including the growth of developing countries and population growth more generally—the demand for Cu has grown rapidly since the turn of the

millennium (Porter and Edelstein, 2003). Currently, demand for Cu is outpacing supply and placing pressure on the discovery of new deposits (Gómez et al., 2007; ICSG, 2016). Meanwhile, discovery rates for Cu-bearing deposits have fallen over time, in part due to rising discovery costs (itself a function of increasing deposit scarcity) (Davies et al., 2021; Schodde, 2020).

Increases in discovery costs are related to the fact that with each new discovery, there is a decrease in the number of deposits that can be detected using conventional exploration techniques such as prospecting, geological mapping and surface geochemistry, all of which are largely surficial exploration tools. This in turn has led to a global rise in the

\* Corresponding author. IsoTropics Geochemistry Lab, Earth and Environmental Science, James Cook University, Townsville, QLD, Australia.

E-mail address: [brandon.mahan@jcu.edu.au](mailto:brandon.mahan@jcu.edu.au) (B. Mahan).

<https://doi.org/10.1016/j.apgeochem.2022.105519>

Received 27 April 2022; Received in revised form 19 October 2022; Accepted 16 November 2022

Available online 23 November 2022

0883-2927/© 2022 The Authors. Published by Elsevier Ltd. This is an open access article under the CC BY-NC-ND license (<http://creativecommons.org/licenses/by-nc-nd/4.0/>).

development and deployment of alternative exploration tools, through geophysics and/or geochemistry, because such methods are capable of detecting economic deposits at depth below the surface (“under cover”) (Schodde, 2020). For critical metals such as Cu, the use of depth-probing exploration tools, along with the decreasing number of deposits that outcrop, has led to an increase in depth of new discoveries (Schodde, 2020). However, and while significant progress has been made in the use and interpretation of such techniques, e.g. for geophysics (Dentith et al., 2018), an impending supply gap—“Peak Copper”—has been forecast if not already reached (WorldBank, 2021).

Summarizing the above, Cu demand and the transition to more sustainable societies call for novel, time- and cost-effective mineral exploration methods capable of detecting economically viable Cu-bearing mineralization under cover. While geophysics has become the go to next-generation exploration method and has shown great utility, it is often logistically and financially non-trivial, especially when involving non-autonomous flyover (Zheng et al., 2021). Furthermore, geophysical surveys such as those relying on electromagnetic properties are not only susceptible to false positives generated by other electromagnetically active materials (e.g. conductive fluids), but their sensitivity decreases with depth and cover thickness. With these caveats in mind, geochemistry has gained traction as a complementary exploration tool. Specifically, hydrogeochemistry of surface and groundwater has gained attention due to its relative ease of deployment and overall cost-efficiency, as the operating cost of such exploration tactics are essentially limited to the cost of conventional fieldwork and subsequent elemental and isotopic analyses. Moreover, such techniques can fill in gaps where methods like geophysics may experience obscuring factors, such that multi-factor survey programs can be designed and deployed.

Hydrogeochemical mineral exploration relies on the premise that hydrolysis and oxidation—weathering—of minerals associated with ore deposits generate multi-element and/or isotopic fingerprints that can be detected by sampling sources of surface and groundwater (artesian springs, well/borehole water). The general expression of this is a trace metal and/or isotopic anomaly proximal to the deposit, which drops off at distance (Kidder et al., 2021, 2022a, 2022b; Mathur et al., 2009a, 2013, 2014). Due to the linkage to chemical reactions at the water-mineral interface, groundwater hydrology and physico-chemical properties (e.g. pH and dissolved oxygen, or dO) can affect the overall manifestation and spatial profile of elemental fingerprints, as can effects of dilution and evaporation (e.g. through meteoric recharge and drought, respectively). Thus, while trace metal abundances (for example) have shown utility in detecting mineralization under cover (e.g. Kidder et al., 2022a), a fundamental caveat of this approach is that trace element profiles are beholden to water-mineral/rock partitioning, itself a strong function of the element profile in the original mineral and the chemical properties of the water; this along with often myriad other variables can prove difficult to de-convolute. As such, trace metal profiles can be highly variable and dependent on the mineralization style present (Eppinger et al., 2013), providing non-unique or duplicitous results that may or may not be indicative of mineralization. With respect to Cu deposit exploration specifically, previous work has also shown that Cu concentrations are not fully representative of proximity to deposit (Mathur et al., 2013). On a separate but important point, many exploration companies conduct their own hydrogeochemical surveys for monitoring and/or exploration purposes that are attached to internal vetting procedures, and therefore concentration data is often proprietary and cannot be readily shared (e.g. for scientific publication).

On the contrary, the same processes that produce elemental anomalies can produce significant mass-dependent isotopic fractionations in trace metals that are unique to their genetic source and/or process, thus allowing for stable metal isotope compositions to be used as genetic fingerprints that can vector to source. While such knowledge has been harnessed by numerous studies in the determination of environmental impacts from mining activities (Fekiacova et al., 2015; Gelly et al., 2019), this tool has seldom been used to vector to ore. To date, there are

only a handful of publications that have indirectly or directly pointed to the utility of stable metal isotopes for vectoring to ore mineralization (Asael et al., 2009; Kidder et al., 2021; Li et al., 2010; Mathur et al., 2005, 2009a, 2013, 2014; Mathur and Wang, 2019). Importantly, and with a specific focus on exploration for Cu-bearing mineralization, the use of hydrogeochemical Cu isotopes in constraining the location of mineralization has shown utility for porphyry, exotic and IOCG (Iron Oxide Copper Gold) Cu-bearing deposit types (Kidder et al., 2021, 2022b; Mathur et al., 2013). This relies on two potentially parallel operating and compounding processes: (i) during weathering of Cu-bearing minerals such as chalcopyrite and chalcocite, the heavy isotope of Cu ( $^{65}\text{Cu}$ ) is preferentially released into solution (relative to  $^{63}\text{Cu}$ ), likely by oxidative weathering (Fernandez and Borrok, 2009; Kimball et al., 2009; Lv et al., 2016; Mathur et al., 2005, 2012); and (ii) preferential adsorption of  $^{65}\text{Cu}$  on precipitates (Balistrieri et al., 2008; Mathur et al., 2013; Pokrovsky et al., 2008). The combined effect of these two processes is the generation of a *bullseye* trend of heavy Cu isotope enrichment—high  $\delta^{65}\text{Cu}$ , or a positive Cu isotope excursion—proximal to mineralization, and a return to background  $\delta^{65}\text{Cu}$  values distal to mineralization (except where extensive carbonates are present) (Mathur and Wang, 2019). While the above provides evidence for the robust use of Cu isotopes in the exploration for Cu-bearing deposits, case studies to date are limited, and as-of-yet have not been applied to any known sediment-hosted copper deposits as ground truth, thus exposing a gap in our understanding of the utility of Cu isotopes in natural waters as a generally applicable exploration tool.

To this end, the current study explores the Cu isotope compositions— $\delta^{65}\text{Cu}$ —of groundwater samples from environmental monitoring bores (18 bores, 1 tailings dam water sample) proximal and distal to the world-class Mount Isa Cu–Zn–Pb deposit (Australia), alongside Cu isotope compositions of 12 chalcopyrite samples from within or very proximal to the main Cu ore body. This case study was conducted to determine the efficacy of Cu isotopes for vectoring to ore using a known sediment-hosted Cu deposit, and furthermore to determine whether Cu isotope compositions can function as an independent and parsimonious vectoring tool, where sample collection and data interpretation alike do not require extensive specialist training.

## 2. Field area and methodology

### 2.1. Brief description of local/regional geology and hydrology

Seven major sedimentary-hosted stratiform Pb–Zn deposits occur within the Paleoproterozoic Mount Isa and McArthur Basins (northern Australia). These include the Mount Isa, Hilton, George Fisher, Dugald River, Lady Loretta, and Century deposits within the Mount Isa Basin, and McArthur River deposit within the McArthur Basin, collectively forming the Australian Proterozoic zinc belt (Cave et al., 2020; Cooke et al., 2000; Leach et al., 2005). The Proterozoic Mount Isa–McArthur basin comprises volcano-sedimentary sequences deposited between 1790 and 1580 Ma during a series of superbasin forming events: the 1790 to 1740 Ma Leichardt Superbasin; the 1730–1640 Ma Calvert Superbasin; and the 1640 to 1580 Ma Isa Superbasin (Gibson et al., 2016). The metasedimentary sequences were variously affected by the 1750 to 1710 Ma Wonga Orogeny (Spence et al., 2021, 2022) and the 1650 to 1490 Ma Isan Orogeny (Abu Sharib and Sanislav, 2013; Foster and Austin, 2008). The local geology is dominated by metasediments of the Mount Isa Group consisting of siltstone, shale, dolomitic shale, sandstone and conglomerate. These were deposited towards the end of the Calvert Superbasin and juxtaposed along the Mount Isa Fault against amphibolite facies rocks deposited in the Leichardt Superbasin (Cave et al., 2020; Gibson et al., 2017). From old to young, the Mount Isa Group consists of the Warrina Park Quartzite (oldest), Moondarra Siltstone, Breakway Shale, Native Bee Siltstone, Urquhart Shale, Spear Siltstone, Kennedy Siltstone and Magazine Shale (youngest). The mineralization is hosted entirely by the Urquhart Shale member, and

terminates at depth against the Paroo Fault (Cave et al., 2020).

In terms of hydrology, the area contains numerous faults and multiple local aquifers of generally low productivity (Buchanan et al., 2020). Regional groundwater flow in the area is influenced by the neighboring Great Artesian Basin, and by host lithologies being strongly fractured and steeply dipping ( $\sim 70^\circ$  west), yielding general indicative regional flow to the N-NE (Buchanan et al., 2020; Herczeg, 2011). Water table levels in the field area range from a few meters (nearest major streams) up to 40+ meters away from major water courses (CBoM, 2022), suggesting complexity at the granular level relative to regional groundwater level estimates (this work; Buchanan et al., 2020). Water table levels are thought to be relatively stable, as the Mount Isa region receives less than 500 mm of precipitation per year, with average precipitation during fieldwork months for this study (February to April) dropping from approximately 90 mm–15 mm (respectively) (Climate-Data.org, 2022), and most rainfall coming from thunderstorms and with rapid run-off (CBoM, 2022).

## 2.2. Field techniques

Groundwater samples were collected by the Environmental Department at Mount Isa Mines (MIM) in 2020 over three field sessions (February, March and April 2020). At the outset of each day, water parameter probes (YSI® *Pro Plus*) were checked/calibrated, and all sampling equipment was cleaned with phosphate-free detergent solutions and deionized (DI) water. Prior to water sample capture, depth to water was measured and bores were purged to a minimum of four bore volumes in order to ensure measurement and collection of fresh/representative groundwater sample from each bore. Water parameters collected in the field include depth to water (m), pH, T (T), dissolved oxygen (DO), and electrical conductivity (EC). After purging, a sufficient volume of water was collected in polypropylene beakers, then filtered using disposable sterile 50 mL syringes (Terumo®) and 30 mm diameter, 0.45  $\mu\text{m}$  cellulose acetate filters (Cameo® 30A). Filtered water samples were collected in pre-cleaned 120 mL clear polypropylene containers (Technoplas™ P10844UU). Syringes were rinsed thrice with sample water prior to filtration, and filters were purged with 5–10 mL of sample water (to purge any contents) prior to collection. Sample containers were filled to overflowing and precautions taken to expel any trapped air prior to sealing. Samples were refrigerated immediately and stored as such until dispatch by courier (on dry ice) to the US for Cu isotope analyses. Upon receipt, samples were acidified with 1 ml of 16 mol/L (molar, or M)  $\text{HNO}_3$ .

Chalcopyrite samples were separated *via* mechanically dislodging and/or micro-drilling grains (as needed) from well-characterized drill cores within and/or directly overlying the main Cu-bearing ore body at Mt Isa. Proximal chalcopyrite location is necessary to provide a representative Cu isotope composition for the primary deposit that minimizes secondary influences, e.g. reservoir Cu isotope effects due to sequential precipitation away from the primary deposit (i.e. Rayleigh distillation of Cu isotopes away from primary deposition) (Mathur and Wang, 2019).

## 2.3. Analytical methods

Approximately 50 g (50 mL) of groundwater was dried in 60 mL Savillex® polyfluoroalkyl (PFA) beakers overnight on a hotplate at 50 °C. For chalcopyrite samples, approximately 1–2 mg of sample was obtained by mechanical separation and/or micro-drilling, then dissolved overnight in *aqua regia*. Copper was purified from dissolved salts with a two stage ion exchange chromatography protocol (Mathur et al., 2013). Full procedural blanks for this method are typically 1 ng Cu or below. The purified salts were then ready for isotopic analysis on the Thermo Fisher Neptune *Plus* MC-ICP-MS instruments at Washington State University and Rutgers University. Analyses were conducted in low resolution wet plasma mode (Mathur et al., 2005). Mass bias was corrected for by sample-standard bracketing (SSB). Samples and standards were

measured at 100 ppb (generating 2.8V on  $^{63}\text{Cu}$ ), and sample voltages matched the standards to within 1V. All data are reported relative to the NIST SRM 976 international Cu standard. The data are presented as  $\delta^{65}\text{Cu}$  values in the conventional per mil (‰) notation, calculated using the following equation:

$$\delta^{65}\text{Cu} = \left[ \frac{\frac{^{65}\text{Cu}}{^{63}\text{Cu}}_{\text{sample}}}{\frac{^{65}\text{Cu}}{^{63}\text{Cu}}_{\text{NIST 976}}} - 1 \right] \times 1000 \text{ (‰)} \quad (1)$$

Samples were measured in duplicate with single blocks of 25 ratios, and on-peak blank measurements were subtracted for each analysis. Errors for the isotope measurements and quality control of the data were assessed in several ways. Errors on measurements for individual samples ( $2\sigma$ , two times the standard deviation) were calculated *via* duplicate analyses, and full procedural replicates were analyzed for approximately 1 in 4 samples to assess long-term and procedural reproducibility; with few exceptions, analytical uncertainties were well below 0.10‰ (Tables 1 and 2). Long-term reproducibility of measurements was further evaluated by comparing standard values to themselves throughout the analytical sessions (Mathur et al., 2005, 2009b). The measured value of the international rock standard BHVO-2 was  $+0.12 \pm 0.06\text{‰}$ , and the measured value of the in-house standard 1838 USA penny was  $-0.02 \pm 0.08\text{‰}$ ; both standard values from the current work are in excellent agreement with literature data (Mathur et al., 2009b; Moynier et al., 2017) (Table 2).

## 3. Results & discussion

### 3.1. Representative Cu isotope signature of Mount Isa Cu–Zn–Pb deposit

A total of 12 chalcopyrite samples were analyzed for their Cu isotope compositions, from two separate drill cores that intersect and/or overly the main ore body (Table 1; Fig. 1). This was done to establish a baseline Cu isotope composition for the deposit, and therefore understand the difference in Cu isotope signature between main Cu-bearing ore and interacting groundwater. The total average Cu isotope composition for the main mineralization of the Mt Isa Cu–Zn–Pb deposit is 0.00‰, noting that there is significant inter-variability due to inherent variations in chalcopyrite Cu isotope composition (not reflective of analytical uncertainties of individual sample analyses, all typically below 0.1‰). Most chalcopyrite Cu isotope compositions lie with 0.2‰ of zero.

### 3.2. Defining industrially impacted groundwater

Tables 1 and 2 report Cu isotope compositions for chalcopyrite and groundwater samples (respectively), along with relevant parameters associated with each. Fig. 2 displays groundwater  $\delta^{65}\text{Cu}$  values overlying a simplified geological map with the Mount Isa orebodies projected to the surface, along with the surface-projected locations of the two drill core lines utilized for chalcopyrite analyses. Duplicate analyses are indicated in Table 2 for groundwater samples; good agreement and low analytical uncertainties confirm sufficient purification of Cu prior to isotopic analyses and robust analytics, especially critical in the case of groundwater samples with high NaCl contents.

Typical electrical conductivity (EC) for freshwater sources range from 100 to 2000  $\mu\text{S}/\text{cm}^2$ , whereas industrial wastewaters have EC values around 10,000  $\mu\text{S}/\text{cm}^2$  (Fondriest Environmental, 2014; Wetzel, 2001). Based on these benchmark values, and previous observations demonstrating that groundwater with electrical conductivity greater than  $\sim 5000 \mu\text{S}/\text{cm}^2$  indicates industrially impacted water (Naudet et al., 2004), this threshold value was set to delineate and discriminate against industrially impacted groundwater. Due to confidentiality consideration for environmental reporting on mining tenements, values at or above this value are not reported herein (however all values have been used for correlative analytics). Specifically within the field area of this work, all

**Table 1**  
Chalcopyrite drill core and Cu isotope data (coordinates in AMG AGD84).

Section	Sample ID	Northing	Easting	From (m)	To (m)	Cu (ppm)	$\delta^{65}\text{Cu}$ (‰)	$2\sigma$
34200N	EX106730	7705759.5	341336.0	575.3	575.4	7760	0.25	0.05
34200N	EX106731	7705759.4	341347.8	595.2	595.3	27200	-0.63	0.09
34200N	EX106732	7705759.0	341380.2	649.2	649.3	9920	-0.14	0.06
34200N	EX106733	7705758.7	341407.9	694.8	694.9	13150	-0.17	0.04
34200N	EX106736	7705758.4	341441.5	749	749.1	1490	0.02	0.06
34200N	EX106737	7705758.4	341459.8	777.7	777.8	6500	-0.06	0.05
35100N	EX089493	7706550.3	341182.0	82.55	82.6	8570	0.16	0.06
35100N	EX089494	7706560.4	341172.5	126.85	126.9	9480	-0.17	0.12
35100N	EX089495	7706554.9	341177.7	102.7	102.75	16500	0.10	0.09
35100N	EX089496	7706553.8	341178.8	97.65	97.7	26100	0.26	0.03
35100N	EX089497	7706548.4	341183.9	73.7	73.75	10400	0.26	0.06
35100N	EX089498	7706543.5	341188.8	51.5	51.55	3190	0.09	0.06
<b>Average</b>							<b>0.00</b>	

**Table 2**  
Borehole Cu isotope data, water parameters and coordinates (AMG AGD84).

Bore ID	$\delta^{65}\text{Cu}$ (‰)	$2\sigma^a$	Depth (m)	Temp (°C)	pH	dO (ppm)	EC ( $\mu\text{S}/\text{cm}^2$ ) <sup>b</sup>	Northing	Easting
2	-0.14	<i>0.06</i> <sup>c</sup>	27.8	29.1	7.11	2.73	1636	7703257	341573
22 <sup>d</sup>	0.00	0.02	4.5	30.1	6.68	1.58	N/A	7702596	335677
29	-5.03	0.09	3.45	29.8	7.69	2.92	N/A	7709466	340929
30	0.63	0.05	22.5	30.5	6.97	2.65	4533	7711460	340677
31	2.10	0.03	40.34	31.3	7.77	5.76	3782	7711807	341953
33	-0.19	<i>0.06</i>	22.6	28.5	6.75	2.56	N/A	7704007	342010
45	2.52	<i>0.03</i>	53.8	30.6	7.08	6.6	2459	7708491	342161
BSOC_A1	-0.11	0.06	1.44	28.1	7.67	2.06	3888	7708847	338749
BSOC_A2	0.94	0.07	1.1	30.1	7.26	2.62	N/A	7708806	338997
BSOC_A3	0.56	0.04	1.71	32.9	7.58	1.26	N/A	7709374	339249
BSOC_A5	3.28	0.09	1.05	31	7.46	6.2	N/A	7710385	340352
BSOC_B4	1.67	0.08	8.28	30.5	7.24	2.39	1684	7709519	339552
BSOC_B5	-1.88	<i>0.11</i>	5.7	31.1	7.16	2.63	N/A	7710206	340131
BSOC_B6	1.53	0.09	7.36	30.2	7.78	2.91	N/A	7710510	340065
NB16	2.11	<i>0.12</i>	3.26	29.2	7.09	1.97	1463	7709920	343066
NB17	1.10	0.10	3	29.2	7.28	1.67	273	7709916	343066
NB21	-0.14	0.05	14.1	31.6	6.94	1.52	2409	7702452	340707
S4	0.09	0.04	3	30.1	7.13	4.31	1735	7702695	335444
TD8 (tailings dam)	2.60	0.03	N/A	30.7	4.59	4.83	N/A	7701187	339281
BHVO-2 (this work)	0.12	<i>0.06</i>							
literature value <sup>e</sup>	0.12								
1838 Penny (this work)	-0.02	<i>0.08</i>							
literature value <sup>f</sup>	0.00								

<sup>a</sup>  $2\sigma$  values calculated from duplicate analyses ( $n = 2$ ) for all samples;  $n = 4$  for BHVO-2 and  $n = 12$  for 1838 USA Penny.

<sup>b</sup> N/A references confidential data (EC > 5000).

<sup>c</sup> Errors in *italics* are for full procedural replicates.

<sup>d</sup> Samples in grey are those with EC > 5000  $\mu\text{S}/\text{cm}^2$ .

<sup>e</sup> Moynier et al. (2017).

<sup>f</sup> Mathur et al. (2009b).

mineralization in the area is hosted within the Urquhart Shale, which does not have evaporite indicators; moreover, the bores along the north-south fault strike (and away from the mine area) do not have elevated EC despite being in the same formation, further indicating no evaporites ("free NaCl") (Neudert, 1983). Indeed, many boreholes on or near tailings dams or mine sites, and/or at shallow depths (<10 m), had EC values greater than 5000  $\mu\text{S}/\text{cm}^2$  and displayed strongly negative and/or erratic  $\delta^{65}\text{Cu}$  values, very likely a consequence of influence from industrial activity in the area. These bores (9) have been interpreted as industrially impacted and have not been included for interpretation with respect to vectoring (demarcated by a grey X in Fig. 2). While these bores have not been included for further interpretation within the

context of Cu isotopes as ore vectoring tools, it is worth noting that all highly negative  $\delta^{65}\text{Cu}$  values within the current work were determined from these industrially impacted bore waters. Thus, while it is not possible to mechanistically constrain these values, as they are likely the result of a melange of potentially co-operative natural and anthropogenic influences (adsorption, biotic/abiotic activity and/or reduction of Cu, introduction of exogenous Cu sources, etc.), these highly negative  $\delta^{65}\text{Cu}$  values do further serve as an empirical indicator of industrial impact. It is further noted that because the presence of soluble evaporites (e.g. NaCl) can increase EC naturally, this is a parameter that should be considered before utilizing EC as a first-order discriminator for industrially impacted water.



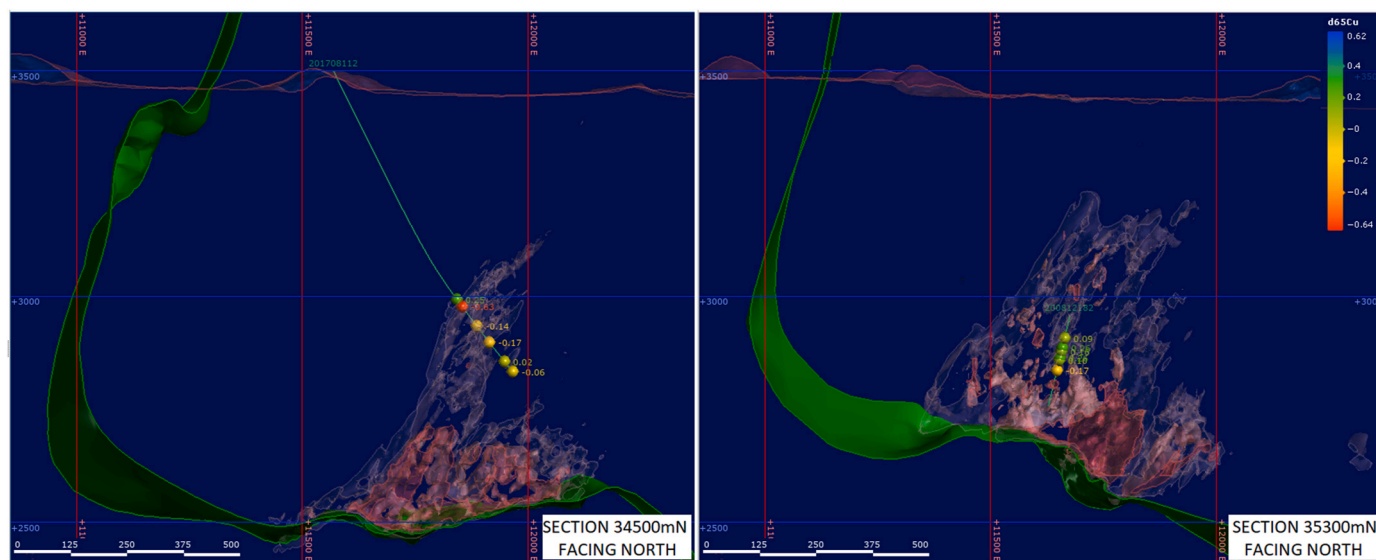


**Fig. 1.** Cross-sectional locations of chalcopyrite samples from drill core sections 34500mN and 345300 mN. Chalcopyrite  $\delta^{65}\text{Cu}$  values reported next to drill core interval and represented by heat index as indicated at right (average  $\delta^{65}\text{Cu}$  and all  $2\sigma$  values reported in Table 2). Green ribbon indicates location of Paroo Fault; red and lavender shading indicates 2% and 0.7% Cu shells (respectively). All chalcopyrite samples are located within or very proximal to the main Cu-bearing orebody. (For interpretation of the references to colour in this figure legend, the reader is referred to the Web version of this article.)

Several of the industrially impacted groundwater samples—especially those near dumps and tailings dams (which contain sulfides)—display elevated  $\delta^{65}\text{Cu}$  values, to be expected given the general process of sulfide weathering as described above. Importantly, this scrutinization of groundwater electrical conductivity indicate that the  $5000\ \mu\text{S}/\text{cm}^2$  threshold acts a strong first-order indicator of adulterated groundwater, which in conjunction with geological context and other parameters (e.g. depth to water) may be used to identify and exclude impacted groundwaters from further interpretation in areas with industrial activity (and without significant evaporites).

### 3.3. Vector signature of unadulterated groundwater

The remaining unadulterated groundwater samples (9 bores) display a clear trend towards higher  $\delta^{65}\text{Cu}$  values in lithologies east of the Mount Isa Fault hosting the Cu ore bodies. Samples proximal to the main ore bodies in the field area have higher  $\delta^{65}\text{Cu}$  values by approximately 1.0–1.5‰ (Table 2, Fig. 2). The tailings dam sample (TD8)—industrially impacted according to the criteria set out above ( $\text{EC} > 5000\ \mu\text{S}/\text{cm}^2$ )—displays a  $\delta^{65}\text{Cu}$  of 2.60‰, in line with that expected for oxidation of Cu sulfides (Mathur et al., 2014).

Correlation matrices were generated for (a) all samples, and (b) only the unadulterated samples (Fig. 3 a,b). When considering all samples alike, weak positive correlations are present for  $\delta^{65}\text{Cu}$ —dO, depth—dO and T—EC (Fig. 3a). Depth—dO and T—EC correlations may be explained by the higher solubility of O at higher pressure (depth), and higher mineral solubility (higher ion content) at higher T (respectively). The weakly positive  $\delta^{65}\text{Cu}$ —dO correlation further supports oxidative weathering as an operative mechanism behind the geo-spatial trend seen in  $\delta^{65}\text{Cu}$  (Fig. 3a), i.e. higher  $\delta^{65}\text{Cu}$  where sulfides are liberating Cu via oxidative weathering (e.g. (Mathur et al., 2018; Plumhoff et al., 2021) and references therein). It is noted that oxygen can be—but is not the only possible—oxidizing species in such reactions, as for example the oxidation of Cu and its release into solution from chalcopyrite weathering can occur due to electron exchange with Fe. This is because stoichiometrically,  $\text{Cu}^+ \text{Fe}^{3+}\text{S}_2^{2-}$  is the dominant species in chalcopyrite (Klekovkina et al., 2014; Zhao et al., 2019), and therefore during dissolution,  $\text{Fe}^{3+}$  can be reduced to  $\text{Fe}^{2+}$ , while  $\text{Cu}^+$  is oxidized to  $\text{Cu}^{2+}$  in the aqueous phase; for this reason, the relationship between  $\delta^{65}\text{Cu}$  and dO is non-binary, again potentially explaining their weak

correlation. When discriminating against industrially impacted (adulterated) samples ( $\text{EC} > 5000\ \mu\text{S}/\text{cm}^2$ ), the weak positive correlations for  $\delta^{65}\text{Cu}$ —dO and depth—dO are enhanced, while that for T—EC diminishes to no correlation; a moderate negative correlation for pH—EC emerges, interpreted as increased solubility of ions at lower pH (Fig. 3b).

### 3.4. Details of individual groundwater bores

Bores NB21, 2, and 33 traverse the Urquhart Shale south of the Cu ore bodies and yield  $-0.14$ ,  $-0.14$ , and  $-0.19\text{‰}$   $\delta^{65}\text{Cu}$  values (Table 2, Fig. 2). These lower  $\delta^{65}\text{Cu}$  values are consistent with the lack of significant Cu mineralization in outcrop or drill samples. Bore 33 ( $\delta^{65}\text{Cu} = -0.19$ ) reported an EC at or above  $5000\ \mu\text{S}/\text{cm}^2$ . This can be explained by the location of this bore hole at the southern end of the Lena prospect, pyrite-rich gossan (Table 2, Fig. 2). The water values might alternatively be explained by drainage down Silver Lena Ck from the 1950's Bernborough Lead mine located 450m NW of this bore. This is perhaps also supported by the relatively low pH of 6.75.

Bore 45 ( $\delta^{65}\text{Cu} = 2.52\text{‰}$ ) is located within the Urquhart Shale within a few hundred meters of gossanous outcrop assaying up to 3000 ppm Cu (Table 2, Fig. 2), thus the strongly positive  $\delta^{65}\text{Cu}$  value is in excellent agreement with the documented mineralization. A significant volume of 180 L was discharged before sampling to ensure pristine groundwater capture.

Bores NB16 and NB17 ( $\delta^{65}\text{Cu} = 2.11$  and  $1.93\text{‰}$ , and  $1.10\text{‰}$ , respectively) are located within the Leichardt River channel (Table 2, Fig. 2). These bores were sampled from a screened interval at 30 m and 40 m depth within the Native Bee Siltstone. As the Cu geochemistry (from auger drill rig bedrock sampling) is well below 65 ppm (Conaghan et al., 2003), it is likely that the  $\delta^{65}\text{Cu}$  values indicate fracture-controlled ground water transported from the south. This is keeping with the inferred groundwater flow direction to the NE (Fig. 2), and this is further supported by the lower  $\delta^{65}\text{Cu}$  of NB16/17 relative to Bore 45.

Bore 31 ( $\delta^{65}\text{Cu} = 2.10\text{‰}$ ) is located on a low ridge of red weathered outcropping Urquhart Shale 3 km north of the mine (Table 2, Fig. 2). Bedrock geochemistry shows  $<65$  ppm Cu and  $>1000$  ppm Zn over a wide area (Conaghan et al., 2003). This bore was sampled from a screened interval at 42 m depth and was probably derived from fracture-controlled ground water that sampled a wide area. Over 400 L of water was discharged before sampling to ensure pristine groundwater

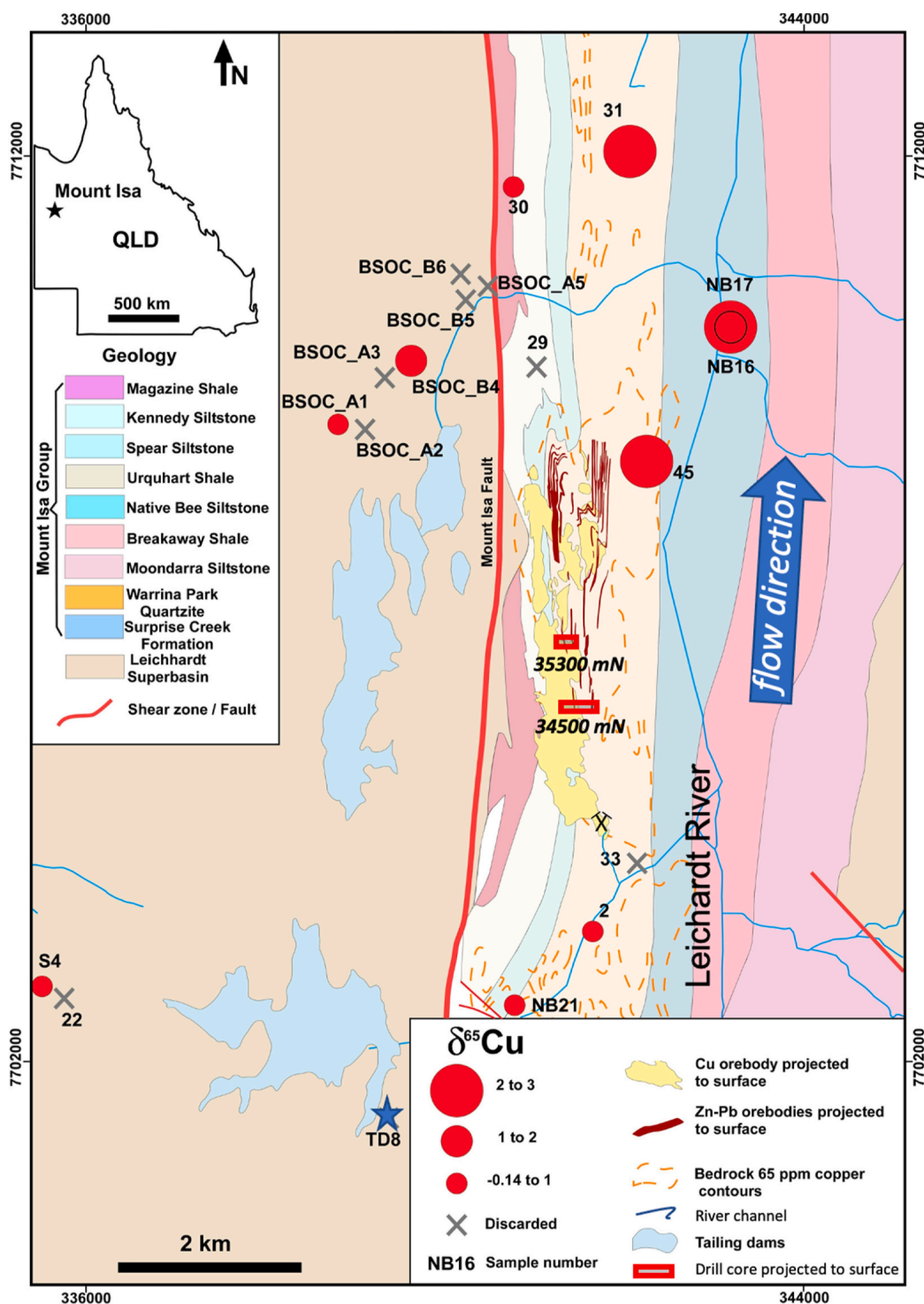


Fig. 2. Spatial distribution of groundwater  $\delta^{65}\text{Cu}$  values from monitoring bores. Values have been superimposed on a simplified geological map of the Mt Isa mine area, including the known ore zones (in red and yellow). Cu isotope compositions ( $\delta^{65}\text{Cu}$ ) for water from bore holes with an EC greater than  $5000 \mu\text{S}/\text{cm}^2$  are indicated by grey Xs and correlate closely with proximity to high-traffic mine sites, and thus are interpreted as industrially impacted. The sample taken directly from the tailings dam is marked by a blue star. Prevailing direction of groundwater flow (NE) is indicated by the blue arrow. All other features are as indicated in legend at bottom right. Moving east of the Mt Isa Fault,  $\delta^{65}\text{Cu}$  values increase with proximity to the mineralization (in bluish red), and prominence of increasing  $\delta^{65}\text{Cu}$  to the NE of the main deposit is indicative of signal carriage by groundwater flow. (For interpretation of the references to colour in this figure legend, the reader is referred to the Web version of this article.)

capture. Result tentatively indicate significant detection of Cu mineralization in the absence of any surface mineralization.

Bore 30 ( $\delta^{65}\text{Cu} = 0.63\text{‰}$ ) is located on Magazine Shale 3 km north of the mine in an area with Cu bedrock concentrations below 65 ppm (Table 2, Fig. 2). The water was taken from 20 to 60 m depth after discharge of 940 L. As the bore is close to the Mount Isa Fault, it is assumed that the water was from fissile fractured formation with substantial north-south flow. The results indicate possible Cu mineralization in the absence of surface mineralization.

Seven bores are located west of the Mount Isa Fault to monitor drainage from the tailings dam and waste dumps reported widely

variable  $\delta^{65}\text{Cu}$  values (both positive and negative) (Table 2, Fig. 2). Five of these bores had EC values at or above  $5000 \mu\text{S}/\text{cm}^2$  and are industrially impacted (bores BSOC\_A2, BSOC\_A3, BSOC\_A5, BSOC\_B4, BSOC\_B5, BSOC\_B6). The most westerly bore BSOC\_A1 returned a  $\delta^{65}\text{Cu}$  value of  $-0.11$  (no anomaly). Bore BSOC\_B4 returned a  $\delta^{65}\text{Cu}$  value of  $1.67\text{‰}$ , suggesting Cu mineralization; however, this bore is only 250 m from a waste dump, and thus has not been interpreted further.

Bores S4 and 22 ( $0.09$  and  $0.00\text{‰}$ , respectively) are located near the south-west edge of Tailings Dam 8 (Fig. 2); S4 does not display an anomalous  $\delta^{65}\text{Cu}$  signature, and 22 has been interpreted as industrially impacted (Table 2).

(a)	$\delta^{65}\text{Cu}$ (‰)	Depth (m)	Temp (°C)	pH	dO (ppm)	EC ( $\mu\text{S}/\text{cm}^2$ )
$\delta^{65}\text{Cu}$ (‰)	1					
Depth (m)	0.197	1				
Temp (°C)	0.170	0.050	1			
pH	-0.235	0.099	-0.008	1		
dO (ppm)	0.442	0.486	0.178	-0.124	1	
EC ( $\mu\text{S}/\text{cm}^2$ )	0.008	-0.315	0.444	0.047	-0.220	1

(b)	$\delta^{65}\text{Cu}$ (‰)	Depth (m)	Temp (°C)	pH	dO (ppm)	EC ( $\mu\text{S}/\text{cm}^2$ )
$\delta^{65}\text{Cu}$ (‰)	1					
Depth (m)	0.260	1				
Temp (°C)	0.318	0.397	1			
pH	-0.374	0.288	-0.256	1		
dO (ppm)	0.575	0.640	0.426	-0.200	1	
EC ( $\mu\text{S}/\text{cm}^2$ )	0.281	-0.014	0.285	-0.656	0.378	1

to colour in this figure legend, the reader is referred to the Web version of this article.)

The tailings dam sample (TD8) was taken directly from Tailings Dam 8 for comparison and is the only non-groundwater sample in the current study (Table 2, Fig. 2). Its  $\delta^{65}\text{Cu}$  of 2.60‰ is in line with that expected from the oxidation of Cu sulfides (Mathur et al., 2014).

### 3.5. Isotopic fractionation of copper

The fractionation of copper in low temperature aqueous solutions has been studied in detail both experimentally and in nature. Fractionation mechanisms of copper include redox changes, biochemical reactions, adsorption and others (Mathur and Wang, 2019). The discussion below outlines the contextual framework for the interpretation of Cu isotope data in groundwater (and surface waters) such as those presented here.

Electron transfer produces the largest measured isotopic shifts in copper. The first experimental studies to show that redox reactions produced isotopic shifts were demonstrated by (Zhu et al., 2002), in which Cu was reduced through laboratory redox-reactions generating isotopic fractionation up to 4‰ (oxidized Cu relative to reduced), and in (Ehrlich et al., 2004), in which the reduction of Cu from solution to produce covellite generated a  $-3\%$  shift of the solution in comparison to the solid material. Oxidation produced a  $+3\%$  shift in the weathering of chalcocite as pointed out by (Mathur et al., 2005), and oxidative weathering more generally produces  $+1.0\text{--}1.5\%$  shift for chalcopyrite (Mathur et al., 2014). Because oxidation of Cu happens routinely above the water table (and in groundwater even in low  $f\text{O}_2$ ), higher Cu isotope compositions in waters are indicative of the presence of Cu sulfide ore regardless of contextual nuances (Borrok et al., 2008; Kimball et al., 2009; Mathur et al., 2005; Plumhoff et al., 2021). Subsequent work in natural waters near known mineral occurrences and acid mine drainage (AMD) corroborate this general concept (Borrok et al., 2008; Kidder et al., 2021; Kimball et al., 2009; Masbou et al., 2020; Mathur et al., 2013, 2014; Pokrovsky et al., 2008; Rodríguez et al., 2013; Roebbert et al., 2018; Viers et al., 2018), wherein the oxidation of Cu sulfides produces higher Cu isotope values (higher  $\delta^{65}\text{Cu}$ ) in comparison to places where no significant oxidation of Cu sulfides exist. The fact that natural and experimental oxidation reactions generate nearly identical isotopic signals indicates that this redox mechanism most likely dominates the Cu isotope composition of the solution when sulfide weathering is involved.

With respect to the current dataset, oxidative weathering of ore

Fig. 3. Correlation matrices for  $\delta^{65}\text{Cu}$  and water parameters. The absolute value of correlation coefficients corresponds to designations:  $0 < [0.4]$  no correlation,  $[0.4]\text{--}[0.6]$  weak correlation,  $[0.6]\text{--}[0.8]$  moderate correlation, and  $> [0.8]$  strong correlation. Blue shading indicates significant positive correlation; green indicates significant negative correlation. (a) When including all data, weak positive correlations were found for  $\delta^{65}\text{Cu}$ —dO, depth—dO and T—EC. (b) When excluding industrially impacted samples ( $\text{EC} > 5000 \mu\text{S}/\text{cm}^2$ ), the weak positive correlations for  $\delta^{65}\text{Cu}$ —dO and depth—dO are slightly enhanced, while that for T—EC is diminished to no correlation; a moderate negative correlation for pH—EC emerges, interpreted as increased solubility of ions at lower pH. Importantly, the persistent (though weak)  $\delta^{65}\text{Cu}$ —dO correlation further validates oxidative weathering of Cu sulfides as the key operative mechanism behind the higher  $\delta^{65}\text{Cu}$  values proximal to the main Cu-bearing ore bodies. (For interpretation of the references

chalcopyrite is strongly supported by the observation that groundwater samples overlying or proximal to the main Cu-bearing mineralization at Mt Isa are shifted to higher  $\delta^{65}\text{Cu}$  by approximately  $1\text{--}2\%$  relative to primary chalcopyrite from the deposit itself (Tables 1 and 2, Figs. 1 and 2) (as are those near the tailings dams containing sulfides).

Other mechanisms involving processes like adsorption and biological reactions can certainly modify Cu isotope values in natural waters, but generally not at the same magnitude as the redox reactions described above. For instance, adsorption will impact solutions at higher pH (e.g.  $\text{pH} > 4$ , the point at which metals will start to adsorb), but this process does not generate the same degree of fractionation ( $< 1\%$  for  $\delta^{65}\text{Cu}$ ) (Balistrieri et al., 2008; Fariña et al., 2018; Li et al., 2015; Liu et al., 2014; Pokrovsky et al., 2008). Biological reactions have been shown to produce several ‰ fractionation, however to overprint the signals produced by oxidative weathering of Cu sulfides, the concentration of bacteria would need to exceed those typically found in nature (Kimball et al., 2009).

## 4. Conclusions & outlook

### 4.1. Impact discrimination, systematics and future work

When deploying Cu isotope systematics in surface and/or groundwater samples, it is of paramount importance to note proximity to potentially industrially impacted sites, as well as to collect standard water parameters—namely EC—in the interest of discriminating against industrially impacted groundwater sampling that can obscure further interpretation. Other parameters such as sampling depth and dissolved oxygen can further aid in interpretation and discrimination of samples. Within the current dataset, prescribing a simple threshold EC of  $5000 \mu\text{S}/\text{cm}^2$ , in conjunction with spatial proximity to risk sites, was sufficient to largely discriminate against industrially impacted waters, thereby allowing for unobscured interpretation of remaining unadulterated water samples.

In the current study, groundwater samples from water bores that occur east of the Mount Isa fault, in lithologies that host the Cu ore bodies, display a clear trend towards strongly positive  $\delta^{65}\text{Cu}$  values (heavier Cu isotope compositions) in proximity to ore relative to more distal  $\delta^{65}\text{Cu}$  values (i.e.  $\delta^{65}\text{Cu}$  values on the order of  $1\%$  heavier or more). Moreover, groundwater  $\delta^{65}\text{Cu}$  values were  $1\text{--}2\%$  heavier than that determined for the main ore body, directly in line with previous



natural and experimental observations (Kidder et al., 2021, 2022b; Mathur et al., 2005, 2013, 2014), and strongly suggesting that oxidative weathering of Cu-sulfides is the key process driving this vector signature. Importantly, while Cu isotope systematics alone cannot discriminate between Cu mineral oxidative weathering from primary ore minerals versus industrially derived inputs (e.g. waste, tailings), this is largely only relevant in contexts such as the current work wherein this potential exploration tool is being validated through deployment in a heavily impacted area with a known and actively mined deposit. The future aim is to deploy hydrogeochemical Cu isotope systematics as a greenfields exploration tool, wherein the fingerprint of industrial activity would be small if not absent altogether, thus alleviating this as a concern. On the other side of this, the current work has additionally shown that Cu isotope systematics can be used in conjunction with other metrics (e.g. EC) to fingerprint industrial input into the local aqueous environment adjacent to extraction activities. Thus, the current work highlights not one, but two uses for Cu isotope systematics in hydrogeochemistry.

Within the study area of the current work, future efforts can look to increase the density of water bore sampling around the mine, particularly within the host lithologies that occur along strike to the north, and to step out towards more distal locations. In a more general sense, future studies should aim to constrain the spatial reach of Cu isotope systematics as an ore vectoring tool, i.e. how far away from mineralization the isotopic anomaly can be detected, and what parameters affect this spatial footprint. Furthermore, more research is needed to understand the effects of seasonality, recharge, groundwater flow rate, aquifer permeability (esp. to meteoric input), etc.

#### 4.2. A straightforward, cost-/time-efficient and generally applicable Cu exploration tool?

Alongside complementary work in different geographic and geological contexts and for differing deposit styles (Kidder et al., 2021, 2022b; Mathur et al., 2013), the results of the current work strongly suggest that hydrogeochemical Cu isotope signatures can be used effectively and across contexts to vector to Cu-bearing mineralization. More precisely, the present work and that of (Kidder et al., 2021, 2022b) suggest that groundwater Cu isotope anomalies can be used to detect Cu-bearing deposits under cover. As discoveries of Cu-bearing deposits have decreased over time, and subsequently new discoveries are moving deeper below the surface, a means to detect mineralization in such contexts is of great value.

The study of (Mathur et al., 2013) includes analyses of economic and non-economic minerals from drill core, and that of (Kidder et al., 2021, 2022b) include an array of other geochemical analyses (e.g. major/trace elements; Mo, S, Sr, O isotopes); in both cases this additional data was used to further contextualize interpretations and spatial relationships to known ore bodies. Such analyses are of great value when it is requisite to determine rock-water relationships, and/or discretize specific mineral assemblages or groundwater reservoirs. However, the results of the current work highlight that in terms of a parsimonious exploration tool, groundwater Cu isotope compositions and standard water parameters collected in the field (namely EC)—alongside an awareness of proximity to risk of industrial influence (and prevailing groundwater flow if known)—are all that is required in order to construct a first-order vector to Cu-bearing ore. Moreover, the current work further illustrates that Cu isotope systematics can be utilized for ore exploration, even where Cu concentrations are either uninterpretable due to conflating factors (as in Section 1) or are inadmissible due to necessary restrictions when conducting analyses on or near industrial sites.

With the above points and caveats in mind, clearly the use of groundwater Cu isotopes as a vectoring tool is still very much in a nascent phase. However, the current work and the few directly comparable studies that exist in the literature (Kidder et al., 2021, 2022b; Mathur et al., 2013) illustrate that groundwater Cu isotope

compositions—thus far—provide a very consistent vector signature that can be used for Cu exploration.

All known data strongly indicate that regardless of geologic context and mineralization type (porphyry, exotic, IOCG and now sediment-hosted), high  $\delta^{65}\text{Cu}$  values relative to background—a relative heavy Cu isotope composition, a.k.a. a positive Cu isotope excursion—indicate proximity to Cu-bearing mineralization. While still in the developmental stage, this line of research calls for further work and potential development in earnest as an exploration tool.

#### Declaration of competing interest

The authors declare the following financial interests/personal relationships which may be considered as potential competing interests: Brandon Mahan, Ioan Sanislav and Paul Dirks report financial support was provided by Mount Isa Mines, Anglo American and Geological Survey of Queensland. Peter Rea reports a relationship with Mount Isa Mines that includes: employment.

#### Data availability

Data will be made available on request.

#### Acknowledgements

BM, IS and PD acknowledge project funding from Mount Isa Mines (MIM) Limited, Anglo American Exploration (Australia) Pty Limited, and the Geological Survey of Queensland (GSQ). The authors would like to thank the Environmental Department at MIM for their support in collecting samples for this project, and the long hours spent pumping/bailing boreholes in excessive heat. The authors also wish to thank the administrative teams at JCU and within its Economic Geology Research Centre (EGRU), and those at MIM and Juniata College, for overseeing the smooth and expeditious dispatch and reception of samples. This study acknowledges the in-kind support of Glencore/MIM and the Geological Survey of Queensland (GSQ), and the financial support of Glencore/MIM, Anglo American and GSQ.

#### References

- Abu Sharif, A.S.A.A., Sanislav, I., 2013. Polymetamorphism accompanied switching in horizontal shortening during isan Orogeny: example from the eastern fold belt, Mount Isa inlier, Australia. *Tectonophysics* 587, 146–167.
- Asael, D., Matthews, A., Oszczepalski, S., Bar-Matthews, M., Halicz, L., 2009. Fluid speciation controls of low temperature copper isotope fractionation applied to Kupferschiefer and Timna ore deposits. *Chem. Geol.* 262, 147–158.
- Balistreri, L.S., Borrok, D.M., Wanty, R.B., Ridley, W.I., 2008. Fractionation of Cu and Zn isotopes during adsorption onto amorphous Fe(III) oxyhydroxide: experimental mixing of acid rock drainage and ambient river water. *Geochem. Cosmochim. Acta* 72, 311–328.
- Borrok, D.M., Nimick, D.A., Wanty, R.B., Ridley, W.I., 2008. Isotopic variations of dissolved copper and zinc in stream waters affected by historical mining. *Geochem. Cosmochim. Acta* 72, 329–344.
- Buchanan, S., Dixon-Jain, P., Martinez, J., Raiber, M., Kumar, P.R., Woods, M., Arnold, D., Dehelean, A., Skeers, N., <Buchanan, CSIRO, 2020. Hydrogeology and groundwater systems of the Isa GBA region. PDF&gt, 2020. In: Geological and Bioregional Assessment: Stage 2. Department of the Environment of Energy, Bureau of Meteorology, CSIRO and Geoscience Australia, Australia.
- Cave, B., Lilly, R., Barovich, K., 2020. Textural and Geochemical Analysis of Chalcopyrite, Galena and Sphalerite across the Mount Isa Cu to Pb-Zn Transition: Implications for a Zoned Cu-Pb-Zn System, vol. 124. *Ore Geology Reviews*.
- CBOM, 2022. Mount Isa Area Climate: Australia. Bureau of Meteorology, Commonwealth of Australia.
- Climate-Data.org, 2022. Climate Mount Isa (Australia): Australia, Climate-Data.Org.
- Conaghan, E.L., Hannan, K.W., Tolman, J., 2003. Mount Isa Cu and Pb-Ag-Zn Deposits of NW Queensland, Australia. *Regolith Expression of Australian Ore Systems*, CRC LEME Geochemistry Regolith Expression of Australian Ore Systems. CRC LEME Geochemistry Special Monograph, p. 3.
- Cooke, D.R., Bull, S.W., Large, R.R., McGoldrick, P.J., 2000. The importance of oxidized brines for the formation of Australian Proterozoic stratiform sediment-hosted Pb-Zn (sedex) deposits. *Econ. Geol.* 95, 1–18.
- Davies, R.S., Davies, M.J., Groves, D., Davids, K., Brymer, E., Trench, A., Sykes, J.P., Dentith, M., 2021. Learning and expertise in mineral exploration decision-making: an ecological dynamics perspective. *Int. J. Environ. Res. Publ. Health* 18.



- Dentith, M., Yuan, H., Johnson, S., Murdie, R., Piña-Varas, P., 2018. Application of deep-penetrating geophysical methods to mineral exploration: examples from Western Australia. *Geophysics* 83, SMJ–Z13.
- Ehrlich, S., Butler, I., Halicz, L., Rickard, D., Oldroyd, A., Matthews, A., 2004. Experimental study of the copper isotope fractionation between aqueous Cu (II) and covellite. *CuS: Chem. Geol.* 209, 259–269.
- Eshkaki, A., Graedel, T.E., Ciacci, L., Reck, B.K., 2016. Copper demand, supply, and associated energy use to 2050. *Global Environ. Change* 39, 305–315.
- Eppinger, R.G., Fey, D.L., Giles, S.A., Grunsky, E.C., Kelley, K.D., Minsley, B.J., Munk, L., Smith, S.M., 2013. Summary of exploration geochemical and mineralogical studies at the giant pebble porphyry Cu-Au-Mo deposit, Alaska: implications for exploration under cover. *Econ. Geol.* 108, 495–527.
- Fariña, A.O., Peacock, C.L., Fiol, S., Antelo, J., Carvin, B., 2018. A universal adsorption behaviour for Cu uptake by iron (hydr) oxide organo-mineral composites. *Chem. Geol.* 479, 22–35.
- Fekiacova, Z., Cornu, S., Pichat, S., 2015. Tracing contamination sources in soils with Cu and Zn isotopic ratios. *Sci. Total Environ.* 517, 96–105.
- Fernandez, A., Borrok, D.M., 2009. Fractionation of Cu, Fe, and Zn isotopes during the oxidative weathering of sulfide-rich rocks. *Chem. Geol.* 264, 1–12.
- Fondriest Environmental, I., 2014. Conductivity, Salinity and Total Dissolved Solids. *Fundamentals of Environmental Measurements*, 2022.
- Foster, D.R.W., Austin, J.R., 2008. The 1800–1610 Ma stratigraphic and magmatic history of the eastern succession, Mount Isa inlier, and correlations with adjacent paleoproterozoic terranes. *Precambrian Res.* 163, 7–30.
- Gelly, R., Fekiacova, Z., Guihou, A., Doelsch, E., Deschamps, P., Keller, C., 2019. Lead, zinc, and copper redistributions in soils along a deposition gradient from emissions of a Pb-Ag smelter decommissioned 100years ago. *Sci. Total Environ.* 665, 502–512.
- Gibson, G.M., Hutton, L.J., Holzschuh, J., 2017. Basin inversion and supercontinent assembly as drivers of sediment-hosted Pb-Zn mineralization in the Mount Isa region, northern Australia. *J. Geol. Soc.* 174, 773–786.
- Gibson, G.M., Meixner, A.J., Withnall, I.W., Korsch, R.J., Hutton, L.J., Jones, L.E.A., Holzschuh, J., Costelloe, R.D., Henson, P.A., Saygin, E., 2016. Basin architecture and evolution in the Mount Isa mineral province, northern Australia: constraints from deep seismic reflection profiling and implications for ore genesis. *Ore Geol. Rev.* 76, 414–441.
- Gómez, F., Guzmán, J.I., Tilton, J.E., 2007. Copper recycling and scrap availability. *Resour. Pol.* 32, 183–190.
- Herczeg, A., 2011. Groundwater. In: Prosser, I.P. (Ed.), *Water: Science and Solutions for Australia*. Australia. CSIRO Publishing, pp. 47–60.
- ICSG, 2016. Copper Bulletin: Preliminary Data for October (enero).
- Kidder, J., Voinot, A., Leybourne, M., Layton-Matthews, D., Bowell, R., 2021. Using stable isotopes of Cu, Mo, S, and <sup>87</sup>Sr/<sup>86</sup>Sr in hydrogeochemical mineral exploration as tracers of porphyry and exotic copper deposits. *Appl. Geochem.* 128, 104935.
- Kidder, J.A., McClenaghan, M.B., Leybourne, M.I., McCurdy, M.W., Pelchat, P., Layton-Matthews, D., Voinot, A., 2022a. Hydrogeochemistry of Porphyry-Related Solutes in Ground and Surface Waters; an Example from the Casino Cu–Au–Mo Deposit, vol. 22. *Exploration, Environment, Analysis, Yukon, Canada: Geochemistry*.
- Kidder, J.A., Sullivan, K., Leybourne, M.I., Voinot, A., Layton-Matthews, D., Stoltz, A., Bowell, R.J., 2022b. Hydrogeochemical mineral exploration in deeply weathered terrains: an example from Mumbwa, Zambia. *Sci. Total Environ.* 810, 151215.
- Kimball, B.E., Mathur, R., Dohnalkova, A.C., Wall, A.J., Runkel, R.L., Brantley, S.L., 2009. Copper isotope fractionation in acid mine drainage. *Geochem. Cosmochim. Acta* 73, 1247–1263.
- Klekovkina, V.V., Gainov, R.R., Vagizov, F.G., Dooglav, A.V., Golovanevskiy, V.A., Pen'kov, I.N., 2014. Oxidation and magnetic states of chalcopyrite CuFeS<sub>2</sub>. A first principles calculation: *Opt Spectrosc.* 116, 885–888.
- Leach, D.I., Sangster, D.F., Kelley, K.D., Ross, R.L., Garven, G., Allen, C.R., 2005. Sediment-hosted Pb-Zn deposits: a global perspective. *Econ. Geol.* 100, 561–608.
- Li, D.L., Sheng-Ao, Li, Shuguang, 2015. Copper isotope fractionation during adsorption onto kaolinite: experimental approach and application. *Chem. Geol.* 396, 74–82.
- Li, W., Jackson, S., Pearson, N., Graham, S., 2010. Copper isotopic zonation in the Northparkes porphyry Cu-Au deposit, SE Australia. *Geochem. Cosmochim. Acta* 74, 4078–4096.
- Liu, S.-A., Teng, F.-Z., Li, S., Wei, G.-J., Ma, J.-L., Li, D., 2014. Copper and iron isotope fractionation during weathering and pedogenesis: insights from saprolite profiles. *Geochem. Cosmochim. Acta* 146, 59–75.
- Lv, Y., Liu, S.-A., Zhu, J.-M., Li, S., 2016. Copper and zinc isotope fractionation during deposition and weathering of highly metalliferous black shales in central China. *Chem. Geol.* 445, 24–35.
- Masbou, J., Viers, J., Grande, J.-A., Freydir, R., Zouiten, C., Seyler, P., Pokrovsky, O., Behra, P., Dubreuil, B., de la Torre, M.-L., 2020. Strong temporal and spatial variation of dissolved Cu isotope composition in acid mine drainage under contrasted hydrological conditions. *Environ. Pollut.* 266, 115104.
- Mathur, R., Falck, H., Belogub, E., Milton, J., Wilson, M., Rose, A., Powell, W., 2018. Origins of Chalcocite Defined by Copper Isotope Values, 2018. *Geofluids*, pp. 1–9.
- Mathur, R., Jin, L., Prush, V., Paul, J., Ebersole, C., Fornadel, A., Williams, J.Z., Brantley, S., 2012. Cu isotopes and concentrations during weathering of black shale of the Marcellus Formation, Huntingdon County, Pennsylvania (USA). *Chem. Geol.* 304–305, 175–184.
- Mathur, R., Munk, L., Nguyen, M., Gregory, M., Anell, H., Lang, J., 2013. Modern and paleofluid pathways revealed by Cu isotope compositions in surface waters and ores of the pebble porphyry Cu-Au-Mo deposit, Alaska. *Econ. Geol.* 108, 529–541.
- Mathur, R., Munk, L.A., Townley, B., Gou, K.Y., Gómez Miguélez, N., Titley, S., Chen, G., Song, S., Reich, M., Tornos, F., Ruiz, J., 2014. Tracing low-temperature aqueous metal migration in mineralized watersheds with Cu isotope fractionation. *Appl. Geochem.* 51, 109–115.
- Mathur, R., Ruiz, J., Titley, S., Liermann, L., Buss, H., Brantley, S.L., 2005. Cu isotopic fractionation in the supergene environment with and without bacteria. *Geochem. Cosmochim. Acta* 69, 5233–5246.
- Mathur, R., Titley, S., Barra, F., Brantley, S., Wilson, M., Phillips, A., Munizaga, F., Maksae, V., Vervoort, J., Hart, G., 2009a. Exploration potential of Cu isotope fractionation in porphyry copper deposits. *J. Geochem. Explor.* 102, 1–6.
- Mathur, R., Titley, S., Hart, G., Wilson, M., Davignon, M., Zlatos, C., 2009b. The history of the United States cent revealed through copper isotope fractionation. *J. Archaeol. Sci.* 36, 430–433.
- Mathur, R., Wang, D., 2019. Transition metal isotopes applied to exploration geochemistry. In: Decrée, S., Robb, L. (Eds.), *Ore Deposits, Geophysical Monograph Series*.
- Moynier, F., Vance, D., Fujii, T., Savage, P., 2017. The isotope geochemistry of zinc and copper. *Rev. Mineral. Geochem.* 82, 543–600.
- Naudet, V., Revil, A., Rizzo, E., Bottero, J.Y., Bégassat, P., 2004. Groundwater redox conditions and conductivity in a contaminant plume from geoelectrical investigations. *Hydrol. Earth Syst. Sci.* 8, 8–22.
- Neudert, M., 1983. A Depositional Model for the Upper Mount Isa Group and Implications for Ore Formation. Australian National University.
- Plumhoff, A.M., Mathur, R., Milovský, R., Majzlan, J., 2021. Fractionation of the copper, oxygen and hydrogen isotopes between malachite and aqueous phase. *Geochem. Cosmochim. Acta* 300, 246–257.
- Pokrovsky, O.S., Viers, J., Emnova, E.E., Kompantseva, E.I., Freydir, R., 2008. Copper isotope fractionation during its interaction with soil and aquatic microorganisms and metal oxy(hydr)oxides: possible structural control. *Geochem. Cosmochim. Acta* 72, 1742–1757.
- Porter, K.E., Edelman, D.L., 2003. Copper statistics. available at: [minerals.usgs.gov/minerals/pubs/of01-006/copper/pdf](https://minerals.usgs.gov/minerals/pubs/of01-006/copper/pdf).
- Rodríguez, N.P., Engström, E., Rodushkin, I., Nason, P., Alakangas, L., Öhlander, B., 2013. Copper and iron isotope fractionation in mine tailings at the Laver and Kristineberg mines, northern Sweden. *Appl. Geochem.* 32, 204–215.
- Roebbert, Y., Rabe, K., Lazarov, M., Schuth, S., Schippers, A., Dold, B., Weyer, S., 2018. Fractionation of Fe and Cu isotopes in acid mine tailings: modification and application of a sequential extraction method. *Chem. Geol.* 493, 67–79.
- Schodde, R.C., 2020. Assessing Long Term Exploration and Discovery Performance for Key Minerals in Australia. MinEx Consulting, Melbourne, Australia.
- Spence, J., Sanislav, I., Dirks, P., 2021. 1750-1710 Ma Deformation along the Eastern Margin of the North Australia Craton: Precambrian Research, vol. 353, 106019.
- Spence, J., Sanislav, I., Dirks, P., 2022. Evidence for a 1750–1710 Ma orogenic event, the Wonga Orogeny, in the Mount Isa Inlier, Australia: Implications for the tectonic evolution of the North Australian Craton and Nuna Supercontinent. *Precambrian Res.* 369, 106510.
- Viers, J., Grande, J.A., Zouiten, C., Freydir, R., Masbou, J., Valente, T., de la Torre, M.-L., Destrigneville, C., Pokrovsky, O.S., 2018. Are Cu isotopes a useful tool to trace metal sources and processes in acid mine drainage (AMD) context? *Chemosphere* 193, 1071–1079.
- Wetzel, R.G., 2001. *Limnology: Lake and River Ecosystems*. Academic Press, San Diego.
- WorldBank, 2021. *Commodity Markets Outlook: Urbanization and Commodity Demand*. October 2021. World Bank, Washington, DC. License: Creative Commons Attribution CC BY 3.0 IGO.
- Zhao, Y., Xue, C., Liu, S.-A., Mathur, R., Zhao, X., Yang, Y., Dai, J., Man, R., Liu, X., 2019. Redox reactions control Cu and Fe isotope fractionation in a magmatic Ni-Cu mineralization system. *Geochem. Cosmochim. Acta* 249, 42–58.
- Zheng, Y., Li, S., Xing, K., Zhang, X., 2021. Unmanned aerial vehicles for magnetic surveys: a review on platform selection and interference suppression. *Drones* 5, 3.
- Zhu, X.K., Guo, Y., Williams, R.J.P., O'Nions, R.K., Matthews, A., Belshaw, N.S., Canters, G.W., de Waal, E.C., Weser, U., Burges, B.K., Salvato, B., 2002. Mass fractionation processes of transition metal isotopes. *Earth Planet Sci. Lett.* 200, 47–62.